

GROUND CHARACTERISATION AND PERFORMANCE OF A SINKING MOTORWAY, WATERVIEW CONNECTION PROJECT, NEW ZEALAND

D.C. Bobei

Managing Director

Addas Ground Engineering Pty. Ltd

Thornleigh, Sydney, NSW, 2120, Australia

ABSTRACT

The paper presents the results and interpretations of an extensive data collected during the procurement phase of SH16 motorway upgrade. The strength and consolidation characteristics are investigated for two prevalent soil units (AH and ATcl). The AH soil is identified to manifest a response which is typical of a sensitive structured soft soil, whereas the ATcl soil is noticed to manifest an over-consolidated behaviour. The estimates based on either CSSM and SHANSEP have limitations to predict undrained shear strength profiles for the sensitive AH soil, but predicting rather well the shear strength of ATcl soil. The undrained shear ratio s_u/σ'_v at $OCR = 1$ for AH soil appears to be a consistent indicator of shear strength development with depth. The non-linear one-dimensional compression displayed by the AH soil is proposed to model using a unique relationship between liquidity index and vertical effective stress. The predictive capability of this relationship is demonstrated by numerical simulations of settlement monitored during the construction and post-construction phase of the original SH16 motorway embankment.

1 INTRODUCTION

1.1 GENERAL

The Western Ring Route (WRR) is an ambitious project initiated by New Zealand Transport Agency (NZTA) to provide a 48km alternative route for improvement of traffic flow around the Auckland city centre. One significant component of the WRR project is the upgrade of the State Highway 16 (SH16), where part of the route is passing through an estuarine environment. This section of the motorway, referred to as the Causeway, has experienced significant settlements over a period of 60 years of service life. Today the traffic lanes are prone to flooding during storm and king tide events.

Under the WRR project scheme, the intent is to: (a) widen the existing motorway with additional traffic lanes to meet the future traffic demand; and (b) to increase to motorway design level to maintain the traffic lanes above the seal level rise. To accomplish the later goal, a great emphasis is placed on: (a) settlement estimates; and (b) rate of settlement accumulation with time for development of whole of life cost estimates for the motorway asset.

1.2 PAPER OBJECTIVES

NZTA has conducted comprehensive investigations of soil conditions along the Causeway Section. The geotechnical investigations included over one hundred exploratory holes, in addition to numerous older holes drilled during the planning phase for the original Causeway in the late 1950s. These investigations have enabled the development of a detailed geological cross-section.

The field investigations are complemented by laboratory testing for the purpose to provide details on strength and compressibility of the Causeway estuarine soil materials. Due to large diversity of estuarine soil types, the paper will focus on differences between two prevalent but different soil units: a structured sensitive soft soil denoted as AH soil unit, and a firm to stiff insensitive soil denoted as ATcl soil.

The compressibility and behaviour of AH and ATcl soils is investigated in the critical state framework. The ability of critical state soil mechanics (CSSM) to predict the undrained shear strength is investigated in comparison with SHANSEP formulation. The predictive capabilities of CSSM and SHANSEP methods are discussed based on the piezometer (CPTu) data.

Based on the non-linear one-dimensional compression manifested by the sensitive AH soil, a framework of analysis is proposed to predict this response. On this basis, an example of soil settlement analysis is carried out to predict the

magnitude and rate of settlement development of the original SH16 motorway embankment during the construction and post-construction stages.

2 GEOLOGICAL CONDITIONS

2.1 GENERAL

A detailed geological model was developed from information collected during five (5) stages of site investigations. A longitudinal model along the centreline part of the motorway is presented in **Figure 1** to illustrate the main stratigraphic units encountered along the Causeway Section. The ground profile consists of geological conditions which adopt a layering code system as summarised in **Table 1**.

Table 1: Geological Layer Codes Adopted in Development of Longitudinal Profile.

Geologic Age	Unit	Layer Code	Description
Late Pleistocene – Holocene	Recent Alluvium	AH	Marine clays and silts – estuarine muds
Pliocene - Pleistocene	Tauranga Group	ATcl*	Clays and Silts
		ATs	Sands and Silty Sands
		ATo/ATp*	Organic Clay/Peat
		ATv	Rhyolitic Silt and Sand (volcaniclastic)
Miocene	East Coast Bay Formation (ECBF)	ER	Residual ECBF Soil
		EW	Weathered ECBF Sandstone – Soil and Rock Fractions (20 < N < 50)
		EU	Unweathered ECBF Rock – Sandstone and Siltstone (N > 50)

*Note: A few of the layer codes are combined to simplify the geology sufficiently to develop an interpretative geological model. In particular, Silts and Clays of the Tauranga Group are combined into a single layer code ATcl, and organic and peats are combined into a single layer code ATo/ATp.

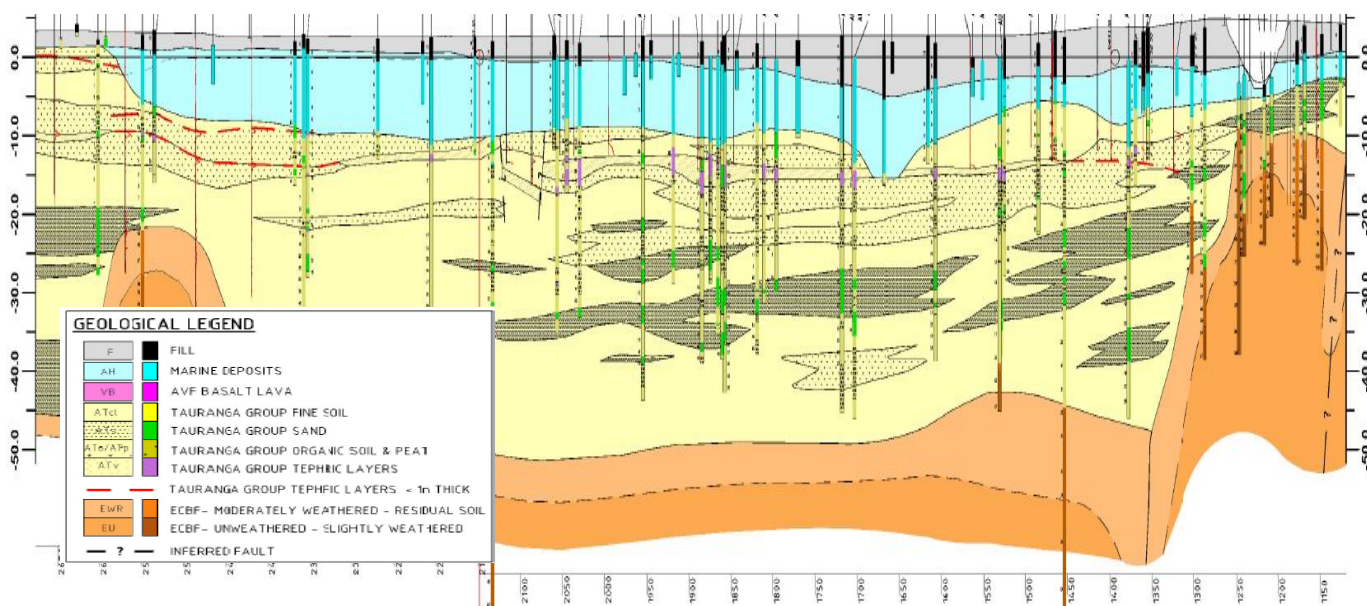


Figure 1: Geological longitudinal section for the Causeway section of SH16 motorway upgrade.

2.2 MARINE SEDIMENTS

The marine sediments belong to the Late Pleistocene-Holocene age (AH) with a deposition environment starting between 8,000 to 14,000 years ago, which still carries on today. The AH deposit generally consists of uniform **Normally Consolidated** Silty Clays. The very soft strength characteristic of the AH soils is in direct contrast to the typically **Overconsolidated** soils present in the underlying Tauranga Group alluvium.

In the Causeway Section, the depth of the Holocene layer varies between 1.5m to 13.0m, generally thinner towards the East (i.e. right hand side in Figure 1) where the ECBF rock head is present at a shallow depth.

2.3 TAURANGA GROUP

The Tauranga Group is of a diverse geological nature developed during the Pliocene-Pleistocene age. It consists of a variety of lithologies accumulated in depositional environments ranging from fluvial to marginal marine. The sequence of soil deposition can be roughly sub-divided into three (3) periods:

1. An initial phase of fluvial deposition → associated with the deposition of basal cohesive sediments (ATcl);
2. A period of fluvial deposition in a more mature and active environment → associated with deposition of discontinuous interbeds of ATo/ATp, ATcl and ATs. The background sedimentation in this environment is the ATcl derived from weathering of hinterland rocks and volcanoclastic sediment resulting in a 'dirty' clay (i.e. silt rich ATcl). Interspersed are organic beds of variable thickness. Some are small (50 to 100m in lateral extent), but thicker organic beds are also present in the deposition environment. There are also three main sand beds in this part of the sequence, as well as multiple minor beds. None of the sands are 'clean' due to presence of a high percentage of fines. The sand beds appear to be irregular in shape, indicating they may be fluvial features associated with migration of an active channel; and
3. A period of active erosion due to rise in relative sea level → associated with deposition followed by erosion of organic dominated sequence from roughly RL -10.0m to -20m. This is thought to coincide with the rise in relative sea level and formation of coastal peat marsh. The organic sequence reaches a maximum thickness of 29.0m in the adjacent Rosebank Peninsula (i.e. left hand side in Figure 1), and it is likely that it continued across the Causeway section prior to being eroded, possibly first by active channel process and later by marine transgression. The Recent Alluvium (AH) was then deposited onto the resulting unconformity. A soil layer which is persistent at roughly -15mRL is a volcanic soil stratum (ATv) associated with the eruptions from the Taupo Volcanic Area. This soil was re-worked and settled through water, and it is typically a fine pumiceous sand and silt with a hard consistency (i.e. SPT blow counts N=50+) causing refusal of CPT probing.

2.4 EAST COAST BAYS FORMATION

The East Coast Bays Formation (ECBF) underlies the entire route. It forms the bedrock for much of Auckland Region (Rock Units EU and EW) with a geological age assigned to the Miocene age (about 26 million years old). The ECBF consists of inter-bedded sandstones and siltstones, which in an unweathered condition is very weak with values of uniaxial confining strength (UCS) between 1 to 3 MPa. Sometimes, the sandstone beds have a lower strength than siltstones, and the sandstone can exist in an un-cemented condition. In the Causeway section, the ECBF lies at great depth between 40 to 50m below the ground level.

3 IN-SITU SHEAR STRENGTH ASSESSMENT

3.1 UNDRAINED SHEAR STRENGTH

The undrained shear strength is an important design parameter, which was assessed by in-situ testing methods such as: (a) shear vanes; and (b) piezocones (CPTu).

The field and hand shear vanes are commonly used to determine the undrained shear strength (s_u) of soft to medium stiff clays. In this project, a typical field vane was used with a diameter of 50 to 65mm and a height to diameter ratio of 2. The hand shear vane was used with a diameter of 25mm and a height of 5mm, with measurements of s_u values taken on the extremities of tube samples collected from the site.

The piezocone testing was conducted using a standard cone: cone angle of 60 degrees, a cross-sectional area of 10 cm², and a porous element located immediately behind the cone. The cone was advanced during field probing at a standard rate of 20mm/sec. The data was measured electronically to include the tip resistance (q_c), sleeve friction (f_s) and the penetration

pore water pressure (u). The cone correction factor (N_k) used to estimate the s_u values, was estimated based on calibrations against the shear vane test results.

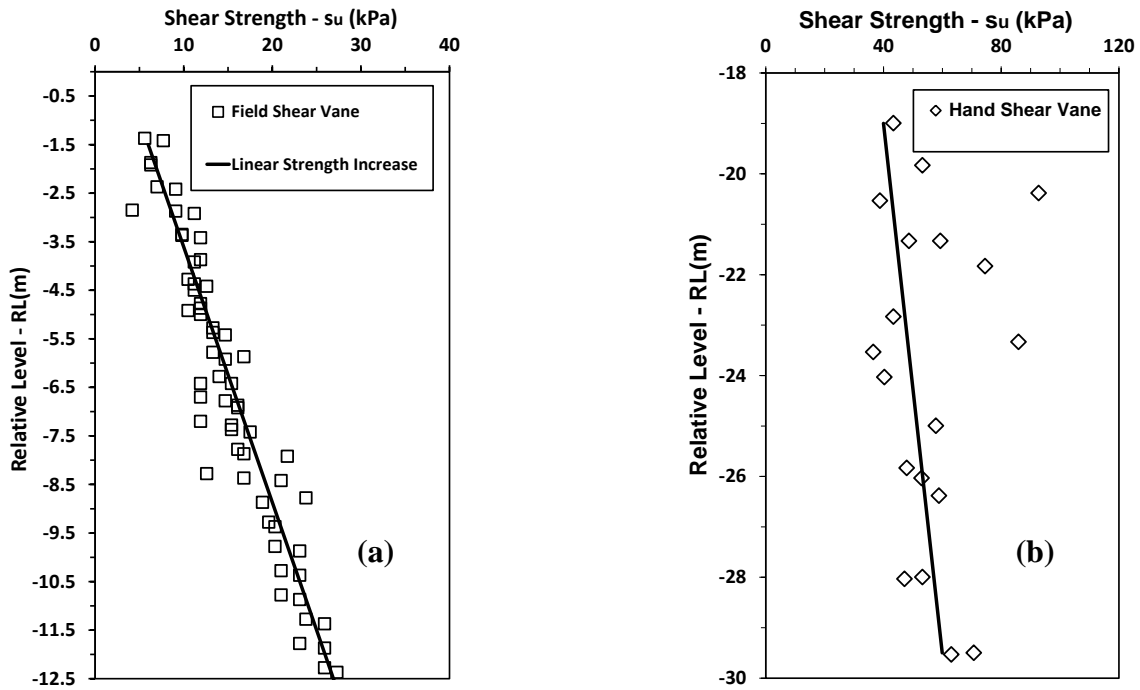


Figure 2: Undrained shear strength profiles: (a) AH soil; and (b) ATcl soil.

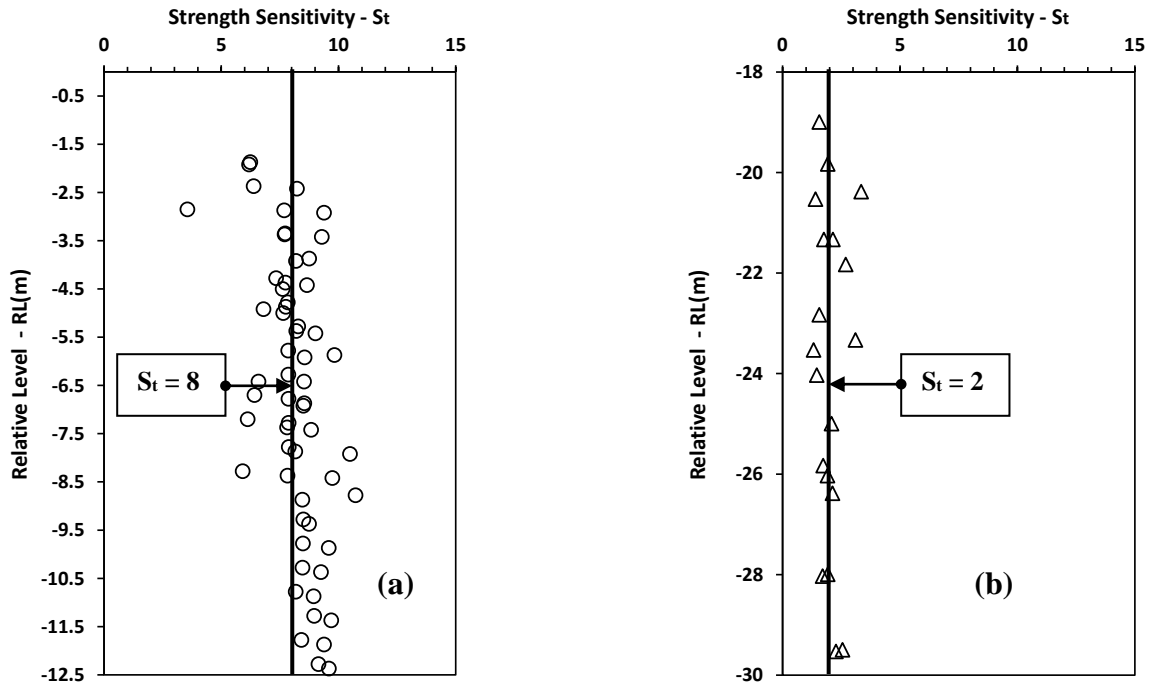


Figure 3: Soil sensitivity: (a) AH soil; and (b) ATcl soil.

The shear vane profiles for both AH and ATcl soils are presented in Figure 2a and 2b. The field shear vane profiles were possible to obtain in the AH soils due to the very soft to soft nature of these soils. Considerable difficulties were

encountered when profiling the deeper ATcl soil, and the strength of ATcl soil was measured by hand shear vanes. The CPTu testing generated a large number of readings, and to avoid clustering the shear strength diagrams these results were chosen not to be included. All shear vane readings were corrected adopting the empirical correction factor (μ) recommended by Bjerrum (1973).

The undrained shear strength is showing an increasing trend with depth in accordance with linear relationships that can be expressed as follows:

1. AH soil for a depth below RL=-1.5m $\rightarrow s_u = 6 + 1.9 \times depth$; and
2. ATcl soil for a depth below RL=-10m $\rightarrow s_u = 30 + 1.7 \times depth$.

3.2 SOIL SENSITIVITY

The soil sensitivity represents an indicator of soil micro-structural bonding or development of inter-particle forces between particles or their aggregates. In this study these effects are referred to as structural bonding. The disturbance to the soil structural bonding during loading could have some serious consequences such as: (a) strength reduction; and (b) changes in the overall soil behaviour due to an increase in soil compressibility properties.

The measure of soil sensitivity (S_t) adopted in this study is based on the ratio between peak undisturbed strength (s_u) and the remould strength (s_r) when soil reaches its residual state. The results of shear vane tests were interpreted to determine the strength sensitivity manifested by AH and ATcl soil as shown in Figures 3a and 3b.

Several classifications of soil sensitivity have been proposed in the technical literature. According to Rosenqvist (1953) the AH soil falls in the range of a Very Sensitive soil (i.e. $4 < S_t < 8$), whereas the ATcl soil can be classified as a slightly sensitive soil material (i.e. $1 < S_t < 2$).

4 EXPERIMENTAL STUDY

4.1 ATTERBERG LIMITS

The consistency limits, liquid limit (LL) and plasticity limits (PL), besides serving the basic means of soil classification, they have also been shown to provide estimates of strength and deformation parameters via empirical correlations: Wroth and Wood (1978), Wroth (1979), Wood (1983), Carrier and Beckman (1984) and Wood (1990).

For this project, the method to assess the LL has largely adopted the “fall cone” method for the AH soils, and Casagrande cup for the ATcl soil. Whilst the fall cone method is recognised to produce consistent and reliable results, Ladeira and Olivera (1995), Leroueil and Le Bihan (1996), a few fall cone determinations were undertaken for the ATcl material to find similar values compared to the Casagrande cup method.

The PL was determined by the method of thread rolling, which is defined according to BS 1377-2:1990 as the moisture content at which a 6mm diameter soil thread rolled between the fingers and a clean glass plate begins to crumble when reduces its diameter to 3mm.

Figures 4 and 5 shows the Atterberg Limits and moisture content determinations for a soil profile at Chainage 1,860m. Of particular interest is the moisture content of AH soil which is found to manifest values higher than LL, slightly decreasing below the LL with depth. The liquidity index (LI) profile for the AH soil is also presented in Figure 4b. The LI values greater than 1 are indicative of a soil micro-fabric that is able to accommodate additional resistance over the remoulded state due to development of structural bonds. The development of structural bonding for the Causeway soft soils has been previously investigated by Newland (1955). A possible cause of structural bonding was attributed to the thixotropic effects due to restoration of soil structure after deposition in a “house of cards” configuration of individual clay particles and aggregations of clay particle groups.

4.2 SAMPLE DISTURBANCE

An evaluation of the soil sample quality is essential, as disturbance may lead to a laboratory measured soil behaviour that is different from its in-situ response. Efforts were made to minimise the sample disturbance, but it inevitably occurs due to stress changes associated with soil sampling. In addition, handling, storage and preparation of soil sample for laboratory testing will further contribute to soil disturbance. Investigations by La Rochelle et al. (1971), Olson (1986) and Terzaghi et

al. (1996) and Lunne et al. (1997), among many others, attributed the sample disturbance to: (a) Damage to the soil structure; and (b) Loss of effective stress.

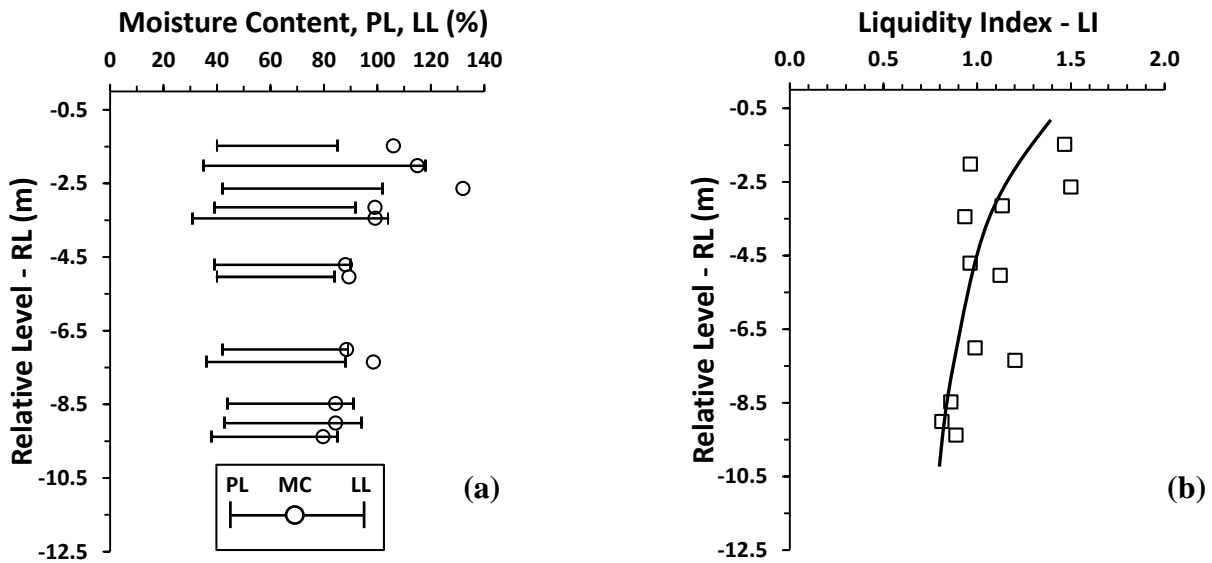


Figure 4: Variation of soil index properties at Chainage 1,860m for AH soil: (a) Atterberg Limits; and (b) Liquidity Index.

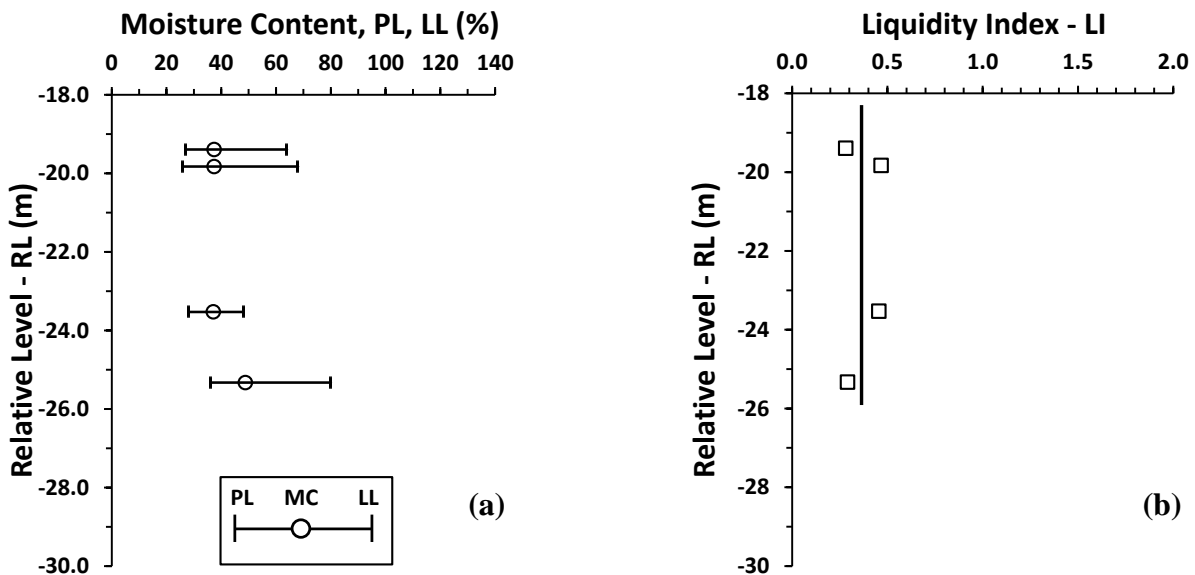


Figure 5: Variation of soil index properties at Chainage 1,860m for ATcl soil: (a) Atterberg Limits; and (b) Liquidity Index.

One of the convenient ways to assess the effects of sample disturbance is based on the soil consolidation properties, as these effects are directly reflected in the shape of the consolidation curve (i.e. flattening of the consolidation curve around the pre-consolidation pressure, σ'_p).

The effects are more pronounced for sensitive clays, as disturbance to the soil structure lowers the void ratio and the associated pre-consolidation σ'_p stress. In this case, the disturbed sensitive soils would be expected to display increased compressibility for stresses smaller than σ'_p , and decreased a compressibility response for stresses higher than σ'_p .

Based on the above considerations, Lunne et al. (1997) proposed to estimate the quality of soil samples based on the ratio $\Delta e/e_0$, where the change in void ratio Δe is measured during soil re-consolidation phase to in-situ vertical stress σ'_{v0} with

consideration of void ratio e_0 at the beginning of this phase. The sample disturbance classification criteria proposed by Lunne et al. (1997) is presented below in Table 2.

Table 2: Proposed criteria for evaluation of soil sample disturbance after Lunne et al. (1997)

$\Delta e/e_0$	Sample Quality
< 0.03	Very Good to Excellent
0.03 – 0.05	Good to Fair
0.05 – 0.10	Poor
> 0.10	Very Poor

Figure 6 presents an assessment of soil sample quality of “reliable” oedometer tests (i.e. sample designation falling in the range of good to excellent). Given the very soft consistency of AH soil, a significant number of samples were found to have an undesirable quality. For brevity and clarity of the paper presentation these values have not been included in Figure 6, and the associated oedometer results have been discarded from further consideration.

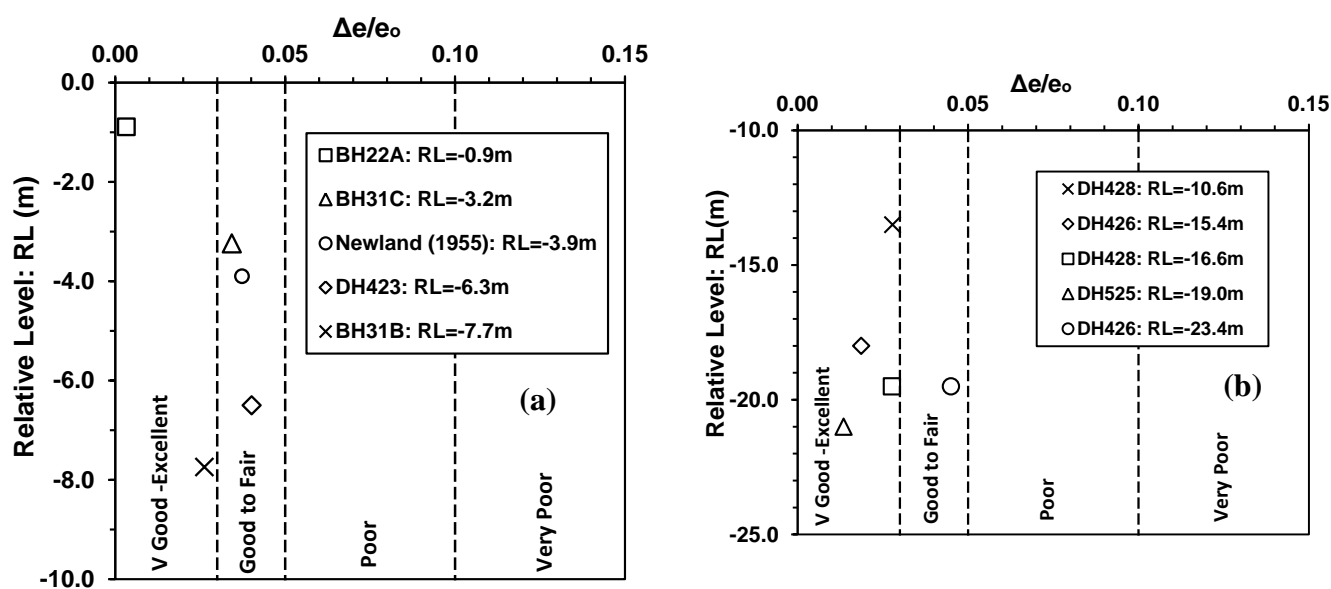


Figure 6: Sample quality classification based on Lunne et al. (1997): (a) AH Soil; and (b) ATcl soil.

4.3 OEDOMETER TESTS

The tests were carried out using a fixed-ring oedometer with drainage allowed at the bottom and the top of the test soil sample. The soil samples were 31mm in diameter and 16mm in height. An incremental loading was applied via a mechanical lever arm capable of applying a vertical effective stress of 3MPa. The settlement of the soil sample was monitored by a Linear Vertical Displacement Transducer (LVDT). Each load increment was applied over a time period of 24 hours, with the end of primary consolidation determined using the square-root-of-time method proposed by Taylor (1942).

All the test samples were cut perpendicular to the direction of in-situ retrieved core axis. A summary of the oedometer testing programme is provided in Tables 3 and 4. For the AH soil, a samples was vigorously remoulded on a glass plate using a spatula to form a soil slurry at a water content equal to the liquid limit. The remoulded soil sample was then transferred/poured into the oedometer ring by tapping the sides to remove any trapped air bubbles.

The results of AH and ATcl oedometer tests are presented in Figures 7a and 7b in a semi-logarithmic plot of void ratio, e , against the logarithm of the vertical effective stress, $\log(\sigma'_v)$. A series of observations are made regarding the results shown in these diagrams as follows:

1. The AH soil compression curves manifest initially a negligible amount of compression before reaching the pre-consolidation stress, σ'_p . When the stress values exceed the pre-consolidation pressure, the consolidation curve displays a non-linear response with a gradient significantly higher compared to the remoulded sample. At high pressures, the compression curve of natural soil is seen to approach the remould consolidation line in an asymptotic trend.
2. Similarly to the AH soil, the compression path of the ATcl material shows initially a negligible amount of compression for stress states below the pre-consolidation stress, σ'_p . However compared to AH soil, σ'_p of ATcl soil is significantly higher. For stresses greater than σ'_p , the compression of ATcl develops along a linear consolidation line.

Table 3: Details of AH soil samples adopted in the programme of one-dimensional compression testing.

Test Name	Sample Type	e_0	MC	PL	LL	σ'_p	s_u/σ'_p
BH22A: RL=-0.9m	Natural Sample	3.160	118	40	90	27.0	0.33
BH31C: RL=-3.2m	Natural Sample	4.127	155	45	110	31.0	0.38
Newland(1955): RL=-3.9m	Natural Sample	3.010	113	38	90	38.4	0.35
DH423: RL=-6.3m	Natural Sample	2.490	93	40	90	55	0.33
BH31B: RL=-7.7m	Natural Sample	3.729	140	44	128	55	0.36
	Remould Sample	2.460	92	40	90	-	-

Table 4: Details of ATcl soil samples adopted in the programme of one-dimensional compression testing.

Test Name	Sample Type	e_0	MC	PL	LL	σ'_p	s_u/σ'_p
DH428: RL=-10.6m	Natural Sample	1.332	50	30	65	180	0.17
DH426: RL=-15.4m	Natural Sample	1.313	49	30	65	180	0.22
DH428: RL=-16.6m	Natural Sample	1.310	49	27	58	220	0.19
DH525: RL=-19.0m	Natural Sample	1.440	54	27	64	250	0.18
DH426: RL=-23.4m	Natural Sample	1.667	62	27	92	250	0.21

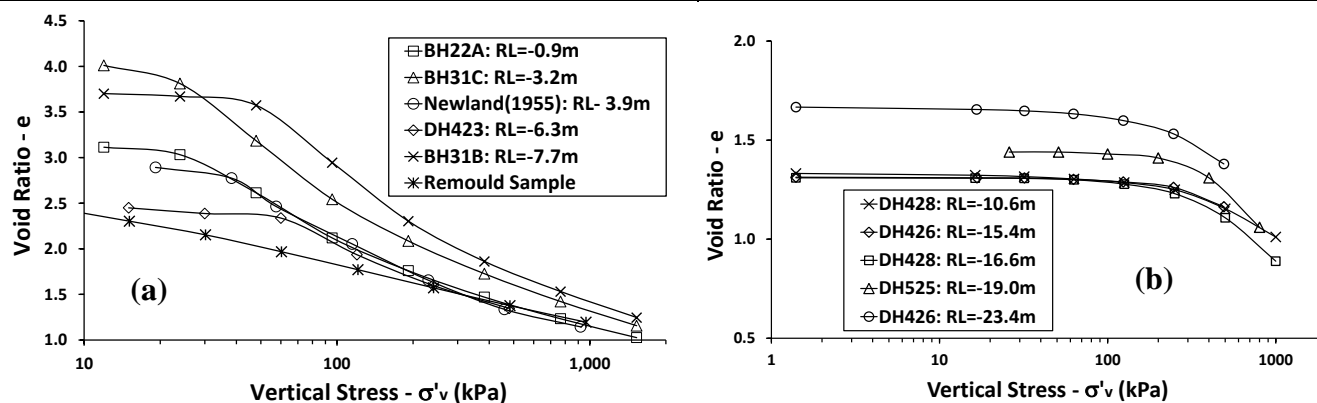


Figure 7: One-dimensional test results: (a) AH soil; and (b) ATcl soil.

4.4 TRIAXIAL TESTS

The triaxial tests were carried out on natural soil samples of diameters varying between 50 and 70mm. For all the tests the sample saturation was achieved in a step by step manner by raising the back pressure to a maximum of 300kPa. Over the duration of saturation, the stress state was maintained at an effective stress of 20kPa. Full saturation was achieved when Skempton's pore pressure parameter B has achieved a value equal or greater than 95%. On completion of soil saturation, the samples were isotropically consolidated before the start of undrained shearing. The undrained shearing was conducted in a deformation controlled mode to large axial strains between 15 to 20%.

An overview of triaxial testing conditions is provided in Tables 5 and 6. Figures 8 and 9 present the results of undrained shearing organised as plots of: (a) effective stress paths \rightarrow deviatoric stress $q = \sigma'_1 - \sigma'_3$ vs. mean effective stress $p' = (\sigma'_1 + 2\sigma'_3)/3$; and (b) stress-strain responses \rightarrow deviatoric stress q vs. axial strain ϵ_1 .

Table 5: Details of AH soil samples adopted in the programme of isotropic undrained triaxial testing.

Test Name	Sample Type	Diameter	Height	e_0	p'_0	p'_{cs}	Comments
DH522: RL=-4.3m	Natural Sample	53	104	1.762	150	-	Not at Critical State
DH503: RL=-4.4m	Natural Sample	73	150	-	300	-	Not Determined
DH525: RL=-5.0m	Natural Sample	53	108	-	75	-	Not Determined

Table 6: Details of ATcl soil samples adopted in the programme of isotropic undrained triaxial testing.

Test Name	Sample Type	Diameter	Height	e_0	p'_0	p'_{cs}	Comments
DH515: RL=-5.0m	Natural Sample	60	112	0.551	50	282	At Critical State
DH710: RL=-8.5m	Natural Sample	60	112	-	200	-	Not Determined
DH516: RL=-9.9m	Natural Sample	60	117	0.908	150	95	At Critical State

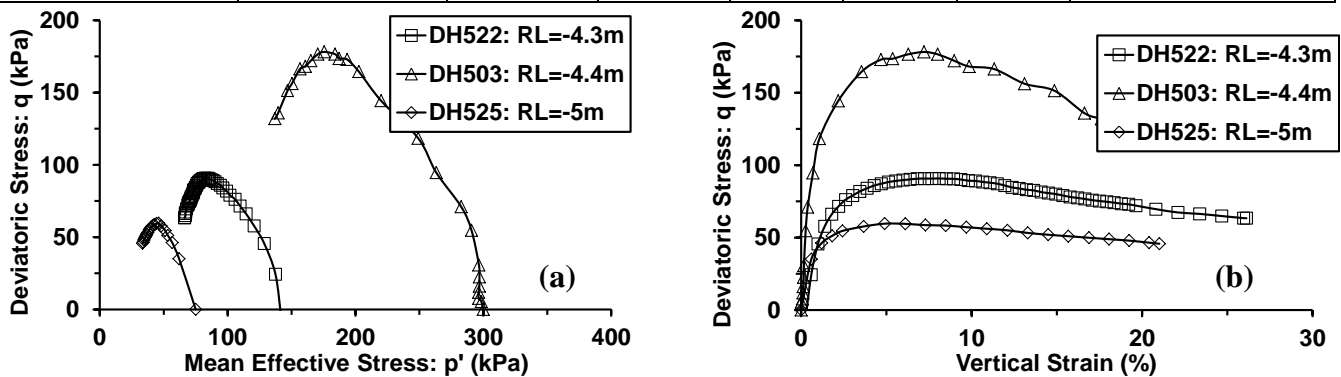


Figure 8: Response of AH soil samples in undrained shearing for a range of confining pressures $p'_0 = 75$ to 300 kPa. (a) Effective stress paths; and (b) Stress-strain relationships.

The behaviour manifested by the AH soil is of a contractive type. The stress paths climb to a maximum deviatoric stress, q_{max} , before plummeting towards the origin of the stress path. The shear strength at q_{max} occurs before the stress paths reach the failure surface (i.e. identified based on $q/p' = \max$ value). The stress-strain diagrams initially show a sharp increase in strength, with the soil stiffness (E_u) showing progressively larger values for shearing commenced from higher confining pressures. The strain softening past q_{max} is a distinctive feature of this suite of tests. It starts from an axial strain of about 5%, and it appears to be more pronounced in undrained shearing conducted from larger confining pressures.

The stress paths of ATcl soil display a strong dilative behaviour. The effective stress paths climb towards the failure surface, and then continue along the failure surface towards the maximum deviatoric stress, q_{max} . Undrained shearing past q_{max} initiates

strain softening, with the stress paths turning towards the origin of the effective stress space.

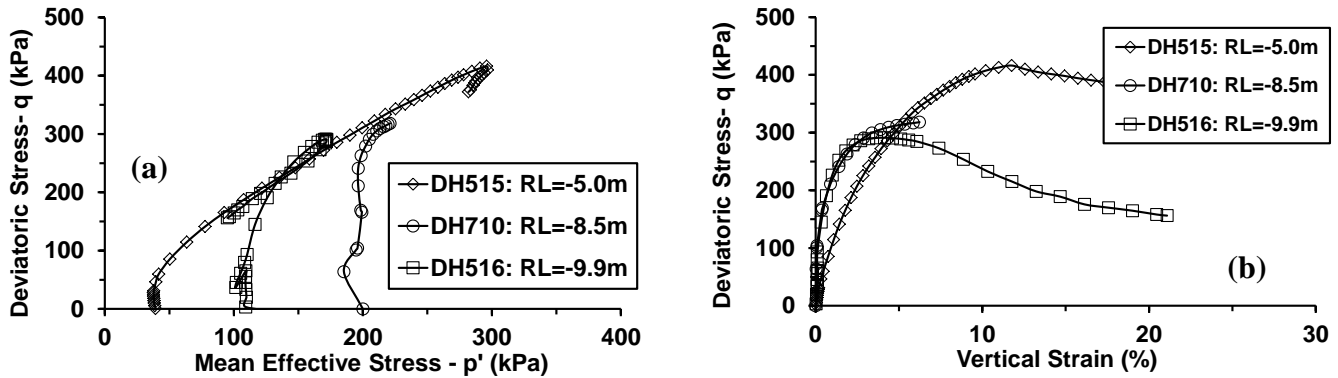


Figure 9: Response of ATcl soil samples in undrained shearing for a range of confining pressures $p'_0 = 45$ to 200 kPa. (a) Effective stress paths; and (b) Stress-strain relationships.

4.5 CRITICAL STATE

The critical state is a fundamental concept in soil mechanics as it represents a reference state to assess the state and behaviour of soil under loading. It was firstly introduced by Roscoe et al. (1958) to describe the behaviour of remoulded clays, and nowadays the concept was extended to represent a more general framework of soil behaviour for: (a) Sands → Been et al (1991); and (b) Combinations of sand with various percentages of plastic and non-plastic fines → Bobei et al. (2009), just to name a few.

The critical state is usually represented in the e - $\log(p')$ plane as a boundary where:

1. Above the CS line (wet side) the soil loading manifests a potential for contraction, which in the case of undrained shearing translates in a potential for development of positive pore water pressure; and
2. Below the CS line (dry side) the soil loading manifests a potential for dilation, which in the case of undrained shearing translates in a potential for development of positive pore water pressure.

The results of undrained triaxial tests conducted on AH and ATcl soils are interpreted in the framework of critical state as illustrated in Figures 10a and 10b. The soil samples were considered to reach the critical state when the following conditions are satisfied: $dq=0$, $dp'=0$, $du=0$ while $d\epsilon_q \neq 0$. The CS for both AH and ATcl is found to plot along a linear relationship, with the CS line for AH soil located above that of the ATcl material. The slope of CS line appears to be steeper for AH compared to ATcl soils, although additional determinations are needed for the ATcl soil to assess the CS at pressures less than 100 kPa.

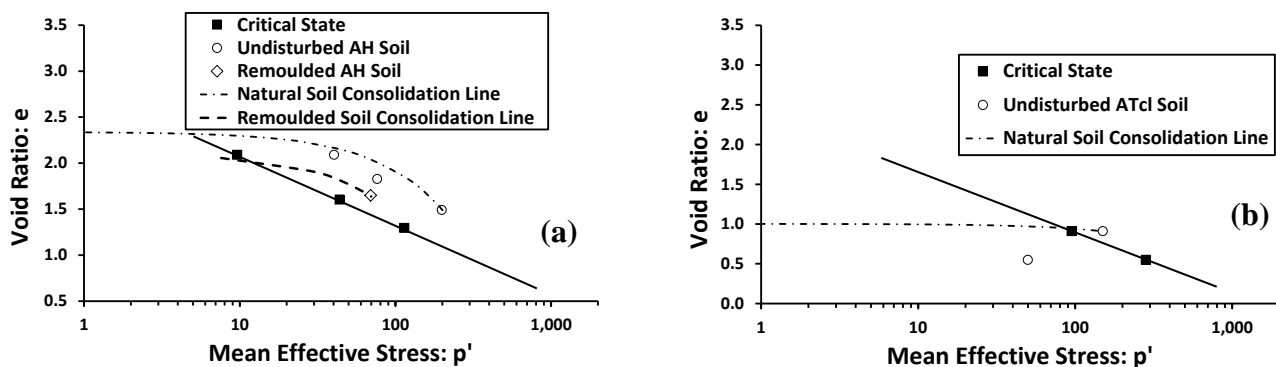


Figure 10: Critical state and soil state of soil before undrained loading: (a) AH soil; and (b) ATcl soil.

Figure 10a illustrates typical isotropic consolidation lines (ICL) and soil states (e_0 and p'_0 shown with open symbols) before undrained shearing for both natural and remould AH soil. The trend of ICL lines is to trace above the CS, with the ICL of natural soil located above that of the remould soil. On consideration that ICL of remould soil is anticipated to follow a

downward trend parallel to the CS line, the natural soil appears to show a tendency to approach the remould line at higher stresses. On the grounds the ICL line is located above the CS line, and the contractive behaviour manifested during undrained loading (refer to Figure 8a), the AH soil appears to fully conform to the framework laid out by CS.

Figure 10b shows a typical ICL line and soil states (e_0 and p'_0 shown with open symbols) of triaxial undrained tests conducted on ATcl material. The soil sample located below the CS (i.e. DH515: RL=-5.0m) shows a dilative response, as otherwise anticipated within the CS framework. The soil sample located above the CS (i.e. DH516: RL=-9.9m) does however manifest a very different behaviour. This test was noticed to commence initially in a dilative manner, but later changed to a contractive response after climbing on the failure surface. The CS has difficulties in providing an explanation for such behaviour.

5 ASSESSMENT OF SHEAR STRENGTH

5.1 SHANSEP AND CRITICAL STATE

SHANSEP (Stress History and Normalised Soil Engineering Properties) was proposed by Ladd and Foot (1974) as an empirical method to adopt in engineering practice to estimate the undrained shear strength on consideration of stress history effects arising from geological unloading. The over-consolidation ratio ($OCR = \sigma'_p/\sigma'_v$) is chosen as a parameter to encapsulate the stress history effects, with the OCR values determined by high quality oedometer data. In mathematical terms, SHANSEP correlates the undrained shear strength with the soil OCR as follows:

$$\frac{s_u}{\sigma'_v} = S \times OCR^m = \left(\frac{s_u}{\sigma'_v} \right)_{OCR=1} \times OCR^m \quad (1)$$

where: S – intercept with vertical axis at $OCR = 1$; and m – gradient of linear relationship.

A study was conducted to obtain a plot of undrained shear strength ratio (s_u/σ'_v) with OCR based on CPTu data. Figures 11a and 11b show these interpretations for AH and ATcl soils. A singular relationship is observed to apply for the ATcl soil, when considering SHANSEP parameters such as: $S = 0.18$; and $m = 1.03$. However, the CPTu data for the AH soil are found to spread over a wider range of values which are contained within the bounds delimited by two linear relationships shown with dashed lines.

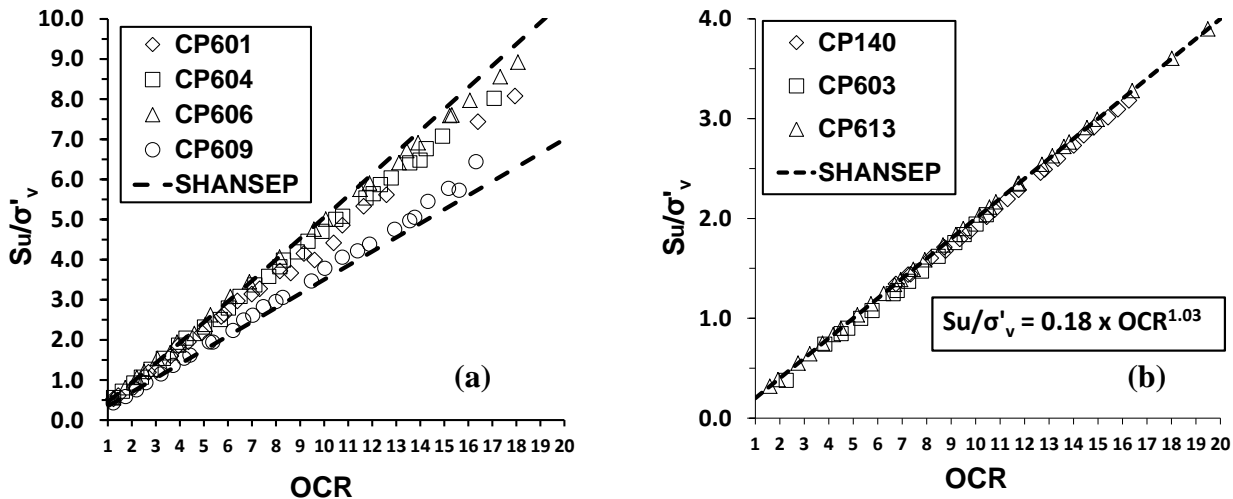


Figure 11: Interpretation of CPTu data by SHANSEP normalisation procedure: (a) AH soil; and (b) ATcl soil.

The variance of SHANSEP relationship deserves further investigation, especially when the behaviour of AH soil was found to comply with the concept of CS. Schofield and Wroth (1968), Roscoe and Burland (1968) and Wood (1990) laid out the foundations of critical state soil mechanics (CSSM) through development of constitutive models such as Cam Clay and Modified Cam Clay. These models seek to capture the behaviour of reconstituted clays on the premise that normalised undrained shear strength (s_u/σ'_v) is numerically correlated with the oedometer compressibility characteristics using a relationship written as:

$$\frac{s_u}{\sigma'_v} = \frac{1}{2} \times \sin(\phi) \times OCR^\Lambda \quad (2)$$

with $\Lambda = 1 - \frac{C_s}{C_c}$, where: C_s is the oedometric swelling index; and C_c is the oedometric compression index.

Inspection of equations (1) and (2) reveal the similarity between the mathematical relationships of SHANSEP and CSSM. A discussion is warranted to better understand these meaning and purpose of the chosen parameters, to allow a better insight into the predictive capability of these relationships. The main points of such discussion are presented below:

(a) The multiplication factors adopted by SHANSEP and CSSM are found to associate with values of:

$$\left(\frac{s_u}{\sigma'_v} \right)_{OCR=1} = 0.33 \rightarrow 0.38 \quad \text{and} \quad \frac{1}{2} \times \sin(\phi) = 0.21 \quad (\text{i.e. } \phi = 25^\circ \text{ at critical state as assessed from triaxial tests}).$$

SHANSEP coefficients are found to retain higher values compared to those predicted by CSSM. The reason for such differences should be viewed in the context of strength sensitive nature AH soil such that: SHANSEP adopts a parameter which considers the s_u at q_{max} , while CSSM considers a reduced undrained shear strength due to strain softening effects (i.e. as a consequence of break-down of the structural bonds during loading as required to achieve the constant void ratio/pore water pressure at CS); and

(b) The power parameters m and Λ , are expected to have a great effect on s_u/σ'_v relationship when $OCR > 1$. These parameters are proposed to embody the compressibility characteristics of AH and ATcl soils. Oedometer data previously presented in Figures 7a and 7b, show fundamental differences between compression behaviour of sensitive AH and insensitive ATcl soils. The general trend for ATcl soil is to manifests a linear compression for $\sigma'_v > \sigma'_p$, compared to AH soil which shows a non-linear response. An additional complication is the curved shape of the consolidation line which appears to change when the AH soil is compressed from different void ratios. The variations in compression characteristics appears to be a likely cause to explain the wide range of strength results observed for AH soil, compared to ATcl material that was noticed to follow a unique linear relationship.

5.2 UNDRAINED STRESS RATIO

SHANSEP methodology using the CPTu data was found to estimate the AH soil undrained stress ratio (s_u/σ'_v) at $OCR = 1$ to lie within a narrow range of values between 0.33 and 0.38. Considering the plasticity index (PI) for AH soil varies between 50 to 60%, these values appear to compare well with the correlation provided by Bjerrum (1972). However an anomaly arises from the fact that the undrained stress ratio reported here is calculated based on corrected shear vane s_u , whereas Bjerrum's chart is presented based on un-corrected s_u values. To provide further validity on the undrained stress ratio determinations for the AH soil, additional values are reported using the oedometer data as summarised in **Table 3**. These values confirm the range of undrained stress ratios assessed based on CPTu interpretations.

6 FRAMEWORK OF SETTLEMENT ANALYSIS

Skempton and Northey (1952) have previously examined the one-dimensional response of a large number of clay soils, suggesting the possibility to develop a correlation between the soil sensitivity and liquidity index. Following on these early comments, the oedometric results of AH soil are interpreted in **Figure 12a** using the Liquidity Index as a normalising parameter.

The various one-dimensional compression curves are observed to “bundle together” in the stress range greater than pre-consolidation stress, σ'_p , with the compression paths converging at higher stresses towards the remould compression line. Such normalisation procedure offers a unique opportunity to model the non-linear one-dimensional compression response using a relationship as follows:

$$\sigma'_v = \frac{LL}{(LI + 0.21)^2} \quad (3)$$

The predictive capability of the proposed mathematical relationship is illustrated in Figures 12a and 12b using the dotted lines. Equation 3 is found to describe very well the one-dimensional compression data in both $LI-\log(\sigma'_v)$, as well as the traditional $e-\log(\sigma'_v)$ space after simple algebraic manipulations to convert LI into a void ratio equivalent.

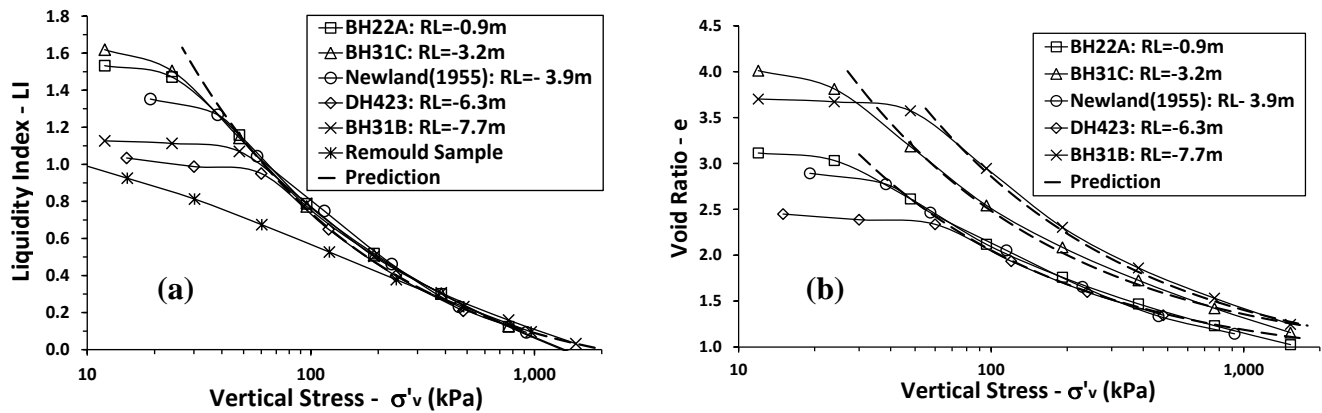


Figure 12: Prediction of non-linear oedometer compression curves for AH soil: (a) LI - σ'_v space; and (b) Traditional e - σ'_v space.

7 EXAMPLE OF SETTLEMENT PREDICTION

7.1 MOTORWAY CONSTRUCTION

The construction of the four lane motorway started in 1951, and it was completed in June 1956. The methodology to build the motorway is shown on historic plans, with additional details provided in Newland and Allely (1952). Due to poor quality of the historic plans, a typical cross-section is re-drawn in Figure 13 to illustrate the configuration of the original embankment.

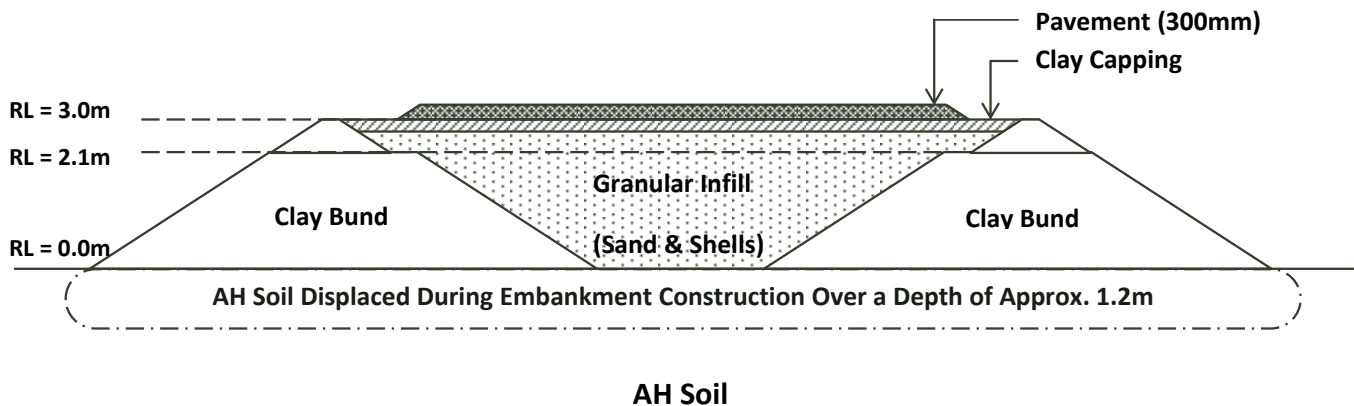


Figure 13: Schematic representation at completion of embankment construction for SH16 motorway in June 1956.

The embankment construction progressed gradually on the surface of soft marine muds to form a series of containment cells, to be later in-filled with granular (sand and shell) and cohesive clay material. The two parallel clay bunds shown in Figure 13 were built in a direction that follows the motorway alignment, spaced at a distance of 25m from each other to create an overall embankment width at the top of 28m. Cross-bunds were built at roughly 100m intervals to complete the containment cells. The bottom clay bunds were built to accommodate at the top a width of 4.5m, and slope gradients of 1:2 (V:H) on the outside and 1:1.5 (V:H) on the inside of the containment cells.

7.2 SETTLEMENT PREDICTION

The settlement prediction for the staged embankment construction was conducted at Chainage 1,860m. An in-house spreadsheet was developed to incorporate the non-linear relationship to describe the compression response of the AH soil.

The main features embedded into the spreadsheet include: (a) Input of a multi-layered soil configuration; (b) Vertical stress increase with depth calculated based on the two-dimensional embankment geometry; (c) Reduction in vertical effective stress due to submergence of fill embankment below the ground water table; (d) Calculation of primary consolidation using Terzaghi's 1-D consolidation theory; and (e) Calculation of creep settlement. A summary table of soil properties adopted in the analyses is provided in Table 7.

Table 7: Details of soil parameters adopted in the settlement predictions.

Soil Unit	γ (kN/m ³)	e_0	C_c	C_r	C_α (NC)	OCR	c_h (m ² /yr)	c_v (m ² /yr)
Marine Alluvium -AH	14.8	2.5 to 3.0	Non-linear Eq. 3	0.110	0.050	1.0m Crust: 5.0+ Deeper: 1.0 to 2.5	1.0	$c_h/1.5$
Tauranga Group - ATcl	17.0	1.3 to 1.4	0.206	0.070	0.011	1.1 to 1.8	5.0	$c_h/2$

The history of fill placement was assumed based on the information presented in the Causeway historic records. It consists of three distinct construction phases, as follows:

1. Phase 1 was completed before June 1952. It includes the placement of a working platform (scoria fill), followed by construction of the bottom clay bunds and infill between the bunds to RL = +2.1m. During this stage, the working platform is shown to have sunk in the soft soil over a depth of 1.2m;
2. Phase 2 running from September 1954 to June 1956. It includes the placement of top clay bund and infill to RL = +3.0m. The last infill layer was placed as a clay capping layer which also forms the pavement subgrade level; and
3. Phase 3 running around June 1956. It includes the construction of the road pavement layers to RL = +3.3m.

Figure 14a shows the historic settlement measurements adopting symbols for comparison with numerical predictions. The monitoring started in June 1952 at completion of Phase 1, but it was discontinued in September 1954 when the construction advanced to Phase 2. The settlement monitoring was resumed in June 1956 to continue for a period of approximately 2 years following the completion of the project. The settlement prediction is shown with a continuous line. The prediction is found to simulate considerably well the magnitude and rate of settlement development with time.

In Figure 14b, the numerical prediction is extrapolated to compare against the settlement measured today (i.e. as shown by the cross symbol). It should be mentioned that the continuous line simulates the development of primary settlement, and the calculation of secondary/creep settlement was also shown with a diamond symbol. A difference in the actual and predicted settlements is estimated to be in the range of 120mm.

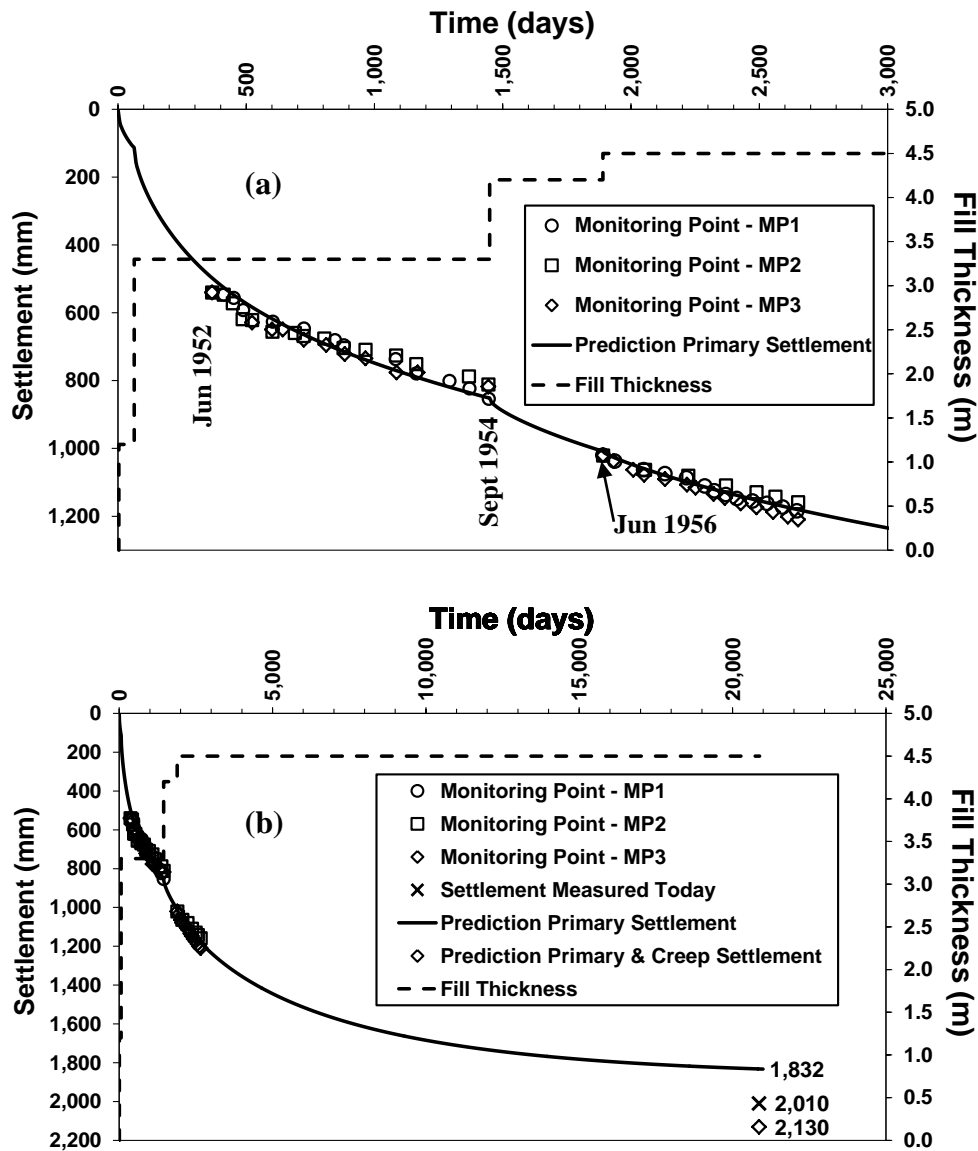


Figure 14: Settlement prediction at centreline of motorway embankment at Chainage 1,860m: (a) During construction and the period of time following embankment completion; and (b) Comparison against settlement measured today.

4 CONCLUSIONS

The paper presents some of the results collected as part of an extensive geotechnical investigation carried out into the sub-surface conditions of the Causeway Section of SH16. Although the Causeway estuarine deposit consists of a wide range of soils, the main focus was set on description of the geotechnical characteristics, namely strength and compressibility, of two essentially different soil types. One type is a normally consolidated sensitive soft soil located in the upper part of the deposit labelled AH soil, and the second type is a deeper over-consolidated insensitive clay and silt labelled ATcl soil. The main findings of the paper are summarised below:

1. The undrained shear strength of both AH and ATcl soils manifests a linear increase with depth. The soil sensitivity remains unaffected by depth retaining values of $S_t = 8$ (i.e. very sensitive) for the AH soil, and $S_t = 2$ (i.e. slightly sensitive) for the ATcl soil.

2. The compressibility of AH soil in one-dimensional testing displays non-linear characteristics when stresses exceed the pre-consolidation pressure, which are significantly higher compared to the remould soil. The behaviour in triaxial testing is of a contractive type, with strain softening manifesting well before reaching the failure condition. The compressibility and undrained behaviour of ATcl soil is typical of a geologically overconsolidated soil.
3. The assessment of undrained shear strength of AH soil is not readily predicted by methods such as SHANSEP and CSSM, which are usually employed in soft soil engineering. The undrained shear ratio s_u/σ'_v at OCR=1 is found to present an alternative method.
4. The one-dimensional response of AH soil is found to uniquely relate the liquidity index and vertical effective stress. The predictive capability of a proposed relationship is demonstrated by numerical simulations of settlement monitored during the construction and post-construction phase of the original SH16 motorway embankment.

5 ACKNOWLEDGEMENTS

The authors wish to express their sincere gratitude for permission given by New Zealand Transport Agency (NZTA) to publish the paper. The extensive site and office work was carried out by a large team of geologists based in the Aurecon Auckland office. Their contribution during the procurement phase of SH16 Causeway Widening project is highly commended. The views expressed in this paper and the interpretations of geotechnical data are those of the author.

6 REFERENCES

- Been, K. and Jefferies, M.G. *A state parameter for sands*. Géotechnique, 1985, **35**(2): pp. 99-112.
- Bobei, D. C., Lo, S. R., Wanatowski, D., Gnanendran, C. T., and Rahman, M. M. *A modified state parameter for characterizing static liquefaction of sand with fines*, Canadian Geotechnical Journal, 2009, **46**(3): pp. 281-295.
- Bjerrum, L. *Embankments on soft ground*. ASCE Conference on Performance of Earth and Earth Supported Structures, Purdue University, 1972, **2**: pp. 1-54.
- Bjerrum, L. *Problems of soil mechanics and construction on soft clays*. Proceedings of 8th International Conference on Soil Mechanics and Foundation Engineering, Moscow, 1973, **3**: pp. 111-159.
- Carrier, W.D. and Beckman, J.F. *Correlations between index tests and properties of remoulded clays*. Géotechnique, 1984, **34**(2): pp. 211-228.
- La Rochelle, P. and Lefebvre, G. *Sampling disturbance in Champlain clays*. Sampling of Soil and Rock, ASTM STP 483, American Society for Testing and Materials, 1971, pp. 143-163.
- Ladd, C.C. and Foot, R. *New design procedure for stability of soft clays*. Journal of Geotechnical Engineering Division, ASCE, 1974, **100**(7): 767-787.
- Ladeira, F.L. and Oliveira, R.E.I *Liquid limits by the BS cone method*. Proceedings of the 11th Europe Conference on Soil Mechanics and Foundation Engineering, 1995, **3**: pp. 139-142.
- Leroueil, S. and Le Bihan, J.P. *Liquid limits and fall cones*. Canadian Geotechnical Journal, 1996, **33**: pp. 793-798.
- Lunne, T., Berre, T. and Strandvik, S. *Sample disturbance on soft low plastic Norwegian clay*. Proceeding of the International Symposium on Recent Developments in Soil and Pavement Mechanics, Rio de Janeiro, Brazil, 1997, pp. 25-27.
- Newland, P. L. and Allely, B.H. *Further evidence of increase of shear strength with depth provided by vane tests on a recent deposit of soft clay*. Proceedings of the 1st Australian-New Zealand Conference on Soil Mechanics and Foundation Engineering, 1952, pp. 123-134.
- Newland, P. L. and Allely, B.H. *Results of site investigations on two sensitive clays*. Proceedings of the 2nd Australian-New Zealand Conference on Soil Mechanics and Foundation Engineering, 1955, pp. 39 - 45.
- Olson, R.E. *State of the art: Consolidation testing, Consolidation of Soils: Testing and Evaluation*. ASTM STP 892, American Society for Testing and Materials, 1986, 7-70.
- Roscoe, K.H, Schofield, A.N. and Wroth, C.P. *On yielding of soils*. Géotechnique, 1958, **8**: pp. 22 - 53.
- Roscoe, K.H. and Burland, J.B. *On the generalized stress-strain behaviour of wet clay*. Engineering Plasticity, Cambridge, 1968, pp. 535-609.

- Rosenqvist, I. Th. *Considerations of the sensitivity of Norwegian quick clays*. Géotechnique, 1953, **3**(5): pp. 195-200.
- Schofield, A.N. and Wroth, C.P. *Critical state soil mechanics*. 1968, McGraw-Hill, London.
- Skempton, A.W. and Northey, R.D. *The sensitivity of clays*. Géotechnique, 1952, **3**: pp. 30-53.
- Taylor, D.W. *Fundamentals of Soil Mechanics*. New York, Wiley Publishers, 1942, pp. 229-239.
- Terzaghi, K., Peck, R.B. and Mesri, G. *Soil mechanics in engineering practice*, 3rd Edition John Wiley Sons, New York, 1996.
- Wood, D. M. *Discussion on cone penetrometer and liquid limit*. Géotechnique, 1983, **33**(1): pp. 76-80.
- Wood, D.M. *Soil behaviour and critical state soil mechanics*. Cambridge University Press, Cambridge, U.K., 1990, pp. 256-308.
- Wroth, C.P. and Wood, D. M. *The correlation of index properties with some basic engineering properties of soils*. Canadian Geotechnical Journal, 1978, **15**(2): pp. 137-145.
- Wroth, C.P. *Correlations of some engineering properties of soils*. Proceedings of the 2nd International Conference on Behaviour of Offshore Structures, London, 1979, **2**: pp. 121-132.